Scientia Iranica B (2011) 18 (5), 1095–1105

SCIENTIA IRANICA

Sharif University of Technology
Scientia Iranica
Transactions B: Mechanical Engineering
www.sciencedirect.com

Design predictive tool and optimization of journal bearing using neural network model and multi-objective genetic algorithm

J. Ghorbanian *, **M. Ahmadi**, **R. Soltani**

Irankhodro Powertrain Company (IPCo), Tehran, Iran

Received 16 November 2010; revised 28 May 2011; accepted 16 July 2011

KEYWORDS
Journal bearing;
Neural network;
Multi objective optimization;
Internal combustion engine;
Genetic algorithm.

Abstract In this paper, rapid and globally convergent predictive tool for dynamically loaded journal bearing design is developed. For accomplishment of such an aim, a neural network model of crankshaft and connecting rod bearings in an internal combustion engine is developed as an alternative for the complicated and time-consuming models. Six most important parameters are selected as inputs of neural network. These parameters are: oil viscosity, engine speed, bearing radial clearance, bearing diameter, slenderness ratio and maximum force applied on bearings. Also, some significant parameters are calculated as neural network outputs. These parameters include: all components of friction loss, all components of oil consumption, minimum oil film thickness, eccentricity, oil temperature rise and displacement relative to shell. In addition, an optimum analysis is performed. To achieve such a target, multi-objective optimization methodology is a good approach inasmuch as several types of objective are minimized or maximized simultaneously. The optimization goal is to minimize friction loss and lubricant flow as the two objectives and develop a Pareto optimal front.

1. Introduction

The behavior of journal bearings is critical to an engine's operation from the point of view of performance and durability. Hence, development of techniques for engine bearing analysis has received extensive attention over the years. With increasing emphasis on the use of simulation methods in engine design, it has become vital to provide engineers with advanced rapid predictive tools for bearing analysis to reduce engine development and analysis times. All analytical and numerical methods developed in this methodology involve solution of the hydrodynamic Reynolds equation for fluid film lubrication. Prior to the appearance of computer simulation methods, simple form solutions were used for the Reynolds equation based on assumptions of "short bearing" and "infinitely long bearing" theories [1,2]. These provided useful design charts for steadily loaded journal bearings.

The available techniques can be categorized into rigorous and rapid techniques [3–5]. The use of finite difference, finite volume or finite element methods [6–9] involve very detailed analysis of bearing geometry. They are probably accurate, but tend to be expensive in skill and time. These methods are confined to researchers. Usually the designers wish to use a less expensive, fairly accurate and easy to understand method, which belongs to the category of rapid methods. In the rapid methods normally one of the three semi-analytical approaches is used to the solution of the dynamic Reynolds equation. These approaches are: short bearing theory, long bearing theory and finite bearing theory.

However, with the advent of computers and the need for analyzing dynamically loaded journal bearings, the mobility method [7,10,11] was developed, which did not involve the direct solution of the Reynolds equation, but used mobility maps. The mobility method is efficient because of the analytical pressure expression and explicit form of the equations of motion. This avoids the need for time consuming iterations involved in the conventional solution of the dynamic Reynolds equation and makes the method very fast. Many researchers worked on mobility method and developed new approaches to optimize its time and accuracy. Goenka [9] presented a set of analytical curve fits, based on Finite Element Method

* Corresponding author.
E-mail address: Jafar.ghorbanian@gmail.com (J. Ghorbanian).

1026-3098 © 2011 Sharif University of Technology. Production and hosting by Elsevier B.V. Open access under CC BY-NC-ND license.
Peer review under responsibility of Sharif University of Technology.

doi:10.1016/j.scient.2011.08.007

Production and hosting by Elsevier

Nomenclature

Cl	radial clearance (μm)
D	bearing diameter (mm)
DS	displacement relative to shell (deg)
DT	oil temperature rise
F	maximum force exerted on bearing (N)
f	total friction loss (Watt)
fp	friction loss due to pressure (Watt)
fo	friction loss due to oil flow (Watt)
fd	friction loss due to damping effect (Watt)
h	journal bearing clearance distribution
IC	Internal Combustion
L	bearing length (mm)
MOFT	Minimum Oil Film Thickness (μm)
MSP	maximum value of shell pressure (MPa)
N	engine speed (rpm)
P	oil film pressure distribution (MPa)
P_{amp}	ambient pressure (MPa)
Q	total oil consumption during one cycle (m^3/s)
QR	oil consumption due to rotation during one cycle (m^3/s)
QS	oil consumption due to squeeze effect during one cycle (m^3/s)
QP	oil consumption due to supply pressure during one cycle (m^3/s)
R	bearing radius (mm)
V_θ	journal rotational velocity (m/s)
V_z	journal axial velocity (m/s)
ε	maximum eccentricity (–)
μ	lubricant viscosity (Pa s)

(FEM) data, to evaluate the mobility vector and maximum pressure. The curve fits are based on statistical analysis and difficulties might therefore be experienced when adapting it to the design of the bearing under consideration. Reason and Narang [12] presented a simple technique for the rapid design and performance evaluation of steady state journal bearings. Hirani et al. [13] extended Reason's approach to dynamically loaded journal bearings, by formulating an analytical pressure expression. He used given force components to determine eccentricity ratios. Therefore, he solved an inverse problem. Stahl and Jacobson [14] determined curve-fitted functions describing each design quantity by following a well-defined procedure. They analyzed three different kinds of geometry and performed an optimum analysis.

In this paper we focused on dynamically loaded journal bearings in which many important bearing operating situations exist. Obviously, in dynamically loaded journal bearings, the load varies in both magnitude and direction. The target is to develop a simulation tool, being able to predict operation parameters of engine crankshaft bearings in a fast and accurate way. After that, the tool will be used to perform optimization on design variables of main and pin bearings of an internal combustion engine.

Artificial Neural Networks (ANNs) which are an emerging tool of artificial intelligence have been shown to be effective in modeling and solving a wide range of complex and nonlinear problems, including many applications to engine and its subsystems modeling [15]. In this research, an ANN modeling was used to calculate journal bearing friction loss, oil consumption, minimum oil film thickness, maximum eccentricity and some

Table 1: Properties of the engine.

Parameter name	Value	Unit
Type	Bi fuel	
Charging method	Natural aspirated	
Cylinder number	4	
Cylinder arrangement	Inline	
Bore	78.6	mm
Stroke	85	mm
Compression ratio	11.05	
Rated. Power	80	kW
Speed @ Rated. Power	6000	rpm
Rated. Torque	136	Nm
Speed @ Rated. Torque	3500	rpm
Main bearing (diameter × width)	50 × 18	mm
Pin bearing (diameter × width)	45 × 18	mm
Main bearing diameter clearance	0.05	mm
Pin bearing diameter clearance	0.05	mm

other important parameters which are required to evaluate design efficacy. Some solved problems of journal bearing calculation are needed to prepare ANN. The one step before ANN preparation is solving the problem of dynamically loaded journal bearing with inputs, which cover the borders of design variable domain.

To optimize the journal bearing design variables at minimum computation efforts, a number of investigations have been done. A paper from Hashimoto [16] provides a good review of work related to journal bearing optimization. In that paper, Hashimoto presented an optimum study for high speed short journal bearings, using successive quadratic programming. Most of the studies [16–18] treat optimization of journal bearings as a continuous variable optimization problem; however, many of the bearing variables are discrete in actual applications. In contrary, Hirani [19], Hirani and Suh [20] and Zengeya and Gadala [21] treat optimization of journal bearings as a discrete variable optimization problem. Hirani [19] analyzed established case studies and showed a significant reduction in friction using thinner viscosity oil. Hirani and Suh [20] continued the work done by Hirani [19], and developed axiomatic design approaches. Zengeya and Gadala [21] used hybrid scheme as an alternative method to that proposed by Hirani and Suh.

In the current paper, simultaneous minimization of flow rate and power loss is targeted due to the conflicting nature of these two objectives and the fact that no single set of design variables can be considered as best for both the objective functions. Moreover, Pareto-optimal front for journal bearing is derived.

In the current research, we attempted to implement exact condition of a recently developed passenger car engine of which the properties are shown in Table 1. Two established case studies at rated power and rated torque are analyzed and viscosity is fixed at critical temperature of engine operation. It should be noticed that according to our climate, the SAE oil 10W40 is used for passenger cars.

The complete method provides very fast, accurate and easy-to-use tool to design optimum bearings for engine crankshaft in early phase of design project. Also, there is high capability to use this method for investigation and research purposes. Overall methodology of the work is illustrated in Figure 1.

2. Hydrodynamic model

The starting point of any fluid-film lubrication analysis is solving the general hydrodynamic Reynolds equation [22], as expressed in Eq. (1), subject to the edge pressure boundary conditions given in Eqs. (2a) and (2b) and the cavitation boundary conditions which are discussed later. The physical description of terms in Eq. (1) is as follows.

The two terms of left hand side are the Poiseuille terms, and describe the net flow rates due to pressure gradients within the lubricated area; the two terms of right hand side are the Couette terms and describe the net entraining flow rates due to surface velocities, and the last term describes the net flow rate due to local expansion.

Where R is the bearing radius, L is the bearing length, V_θ is the journal rotational velocity, V_Z is the journal axial velocity, μ is the lubricant viscosity, $h(\theta, z)$ is the journal bearing clearance distribution, $P(\theta, z)$ is the oil film pressure distribution in the clearance zone, and P_{amb} is the ambient pressure at the bearing edges.

Within the code, oil film pressures are calculated by finite difference solution. A brief description of this method is given in the following section.

2.1. Finite-difference solution

A rigorous solution to the lubrication equation shown in Eq. (1) is obtained, using finite-difference techniques. In this approach, the governing Reynolds equation is discretized in time and space using finite difference operators such as:

$$\frac{1}{R^2}\frac{\partial}{\partial\theta}\left(\frac{h^3}{12\mu}\frac{\partial P}{\partial\theta}\right)+\frac{\partial}{\partial z}\left(\frac{h^3}{12\mu}\frac{\partial P}{\partial z}\right) = \frac{V_\theta}{2R}\frac{\partial h}{\partial\theta}+\frac{V_z}{2}\frac{\partial h}{\partial z}+\frac{\partial h}{\partial t}. \tag{1}$$

B.C's:

$$@z = 0, \qquad P = P_{amb}, \tag{2a}$$

$$@z = L, \qquad P = P_{amb}, \tag{2b}$$

$$\left(\frac{\partial P}{\partial\theta}\right)_{i,j}^{t} = \frac{P_{i,j+1}^{t} - P_{i,j-1}^{t}}{2\Delta\theta},$$

$$\left(\frac{\partial h}{\partial\theta}\right)_{i,j}^{t} = \frac{h_{i,j+1}^{t} - h_{i,j-1}^{t}}{2\Delta\theta},$$

$$\left(\frac{\partial P}{\partial z}\right)_{i,j}^{t} = \frac{P_{i+1,j}^{t} - P_{i-1,j}^{t}}{2\Delta z},$$

$$\left(\frac{\partial h}{\partial z}\right)_{i,j}^{t} = \frac{h_{i+1,j}^{t} - h_{i-1,j}^{t}}{2\Delta z},$$

and:

$$\left(\frac{\partial h}{\partial t}\right)_{i,j}^{t} = \frac{h_{i,j}^{t} - h_{i,j}^{t-\Delta t}}{\Delta t}.$$

The nodal Reynolds equations lead to a set of linear algebraic equations of the form $[K]\{P\} = \{R\}$, where $[K]$ is the coefficient matrix associated with the column of unknown oil film pressures $\{P\}$ and $\{R\}$ is a column of known terms, which are on the right hand side of Eq. (1). The oil film pressures are then solved, using the Gaussian elimination method. The solution process described above permits negative values of oil film pressure. They are considered to correspond to the cavitating nodes in the bearing clearance zone. As a result, the oil film pressure values are post-processed whereby all negative and sub cavitation pressures are reset to a constant cavitation pressure value.

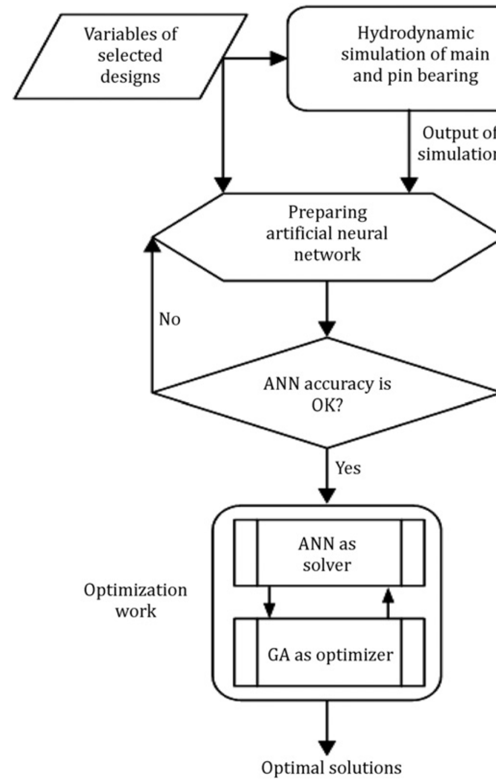

Figure 1: Overall flowchart of the work.

3. Artificial neural network

Feed-forward networks are a common type of neural networks [23]. A feed-forward network comprises an input layer, where the inputs of the problem are received, hidden layers, where the relationship between the inputs and outputs are determined and represented by synaptic weights, and an output layer which emits the outputs of the problem. The neural feed-forward network is modeled with three basic elements:

(a) A set of synapses characterized by synaptic weights.
(b) An adder or linear combiner for summing the input signals.
(c) An activation function for limiting the amplitude of the output of a neuron to some finite value.

The input of the activation function can be increased by using a bias term [24–28]. Here, we have made use of a certain ANN architecture known as the multi-layer feed-forward neural network or Multi Layer Perceptron (MLP). The schematic of Figure 2 shows the model of a neuron, which forms the basis of designing neural networks.

Here, p is an R length input vector, W is an $S \times R$ matrix, and a and b are S length vectors. As defined previously, the neuron layer includes the weight matrix, the multiplication operations, the bias vector b, the summer and the activation function boxes.

3.1. ANN development and implementation

In this work, both ANN implementation and training was developed, using the neural network toolbox of MATLAB. Different ANNs were built rather than using one large ANN including all the output variables. This strategy allowed for better adjustment of the ANN for each specific problem, including the optimization of the architecture for each output [26]. The list of outputs and inputs are shown in Tables 2 and 3, respectively.

Table 2: List of outputs.

Outputs	Definition	Units
ε	Maximum eccentricity (lower and upper shell)	–
DS	Displacement relative to shell (lower and upper shell)	deg
MOFT	Minimum oil film thickness (lower and upper shell)	µm
QR	Oil consumption due to rotation during one cycle	Liter/min
QS	Oil consumption due to squeeze effect during one cycle	Liter/min
QP	Oil consumption due to supply pressure during one cycle	Liter/min
fp	Friction loss due to pressure	Watt
fo	Friction loss due to oil flow	Watt
fd	Friction loss due to damping effect	Watt
MSP	Maximum value of shell pressure	MPa

Table 3: List of inputs.

Inputs	Definition	Range of variation	Units
N	Engine speed	1500–6000	rpm
μ	Oil viscosity	0.006–0.086	Pa s
F	Maximum force exerted on bearing	8000–14000	N
Cl	Radial clearance	7–37	µm
D	Bearing diameter	36–64	mm
L/D	Slenderness ratio	0.25–0.5	–

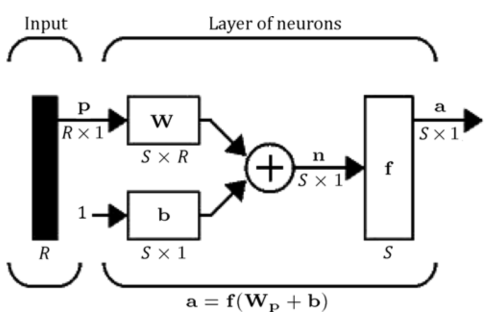

Figure 2: Basic structure for multi-layer perceptron network.

For every set of engine speed, oil viscosity and maximum force exerted on bearings, a network is trained with *Cl*, *D* and L/D ratio as inputs. 1858 samples are applied for training, validating and testing in each set of data. For each ANN, the input layer uses 6 nodes and the output layer uses 1 node. The selection of the exact number of hidden layer and number of neurons in each hidden layer for each output was based on the accuracy of results, following a trial and error procedure. This adjustment allowed the complexity of the modeled phenomenon to be taken into account. The number of neurons evaluated ranged from 1 to 20, which avoided large number of weights to be adjusted in the training process for the available patterns. Also, the same number of neurons is selected for two hidden layers. In the trial and error procedure, the accuracy of the ANN prediction results was compared and the best architecture was selected. Some outputs of main bearing No. 1 is presented in Table 4.

The activation functions chosen were sigmoids for the hidden neurons as they allowed nonlinear relationships between inputs and outputs and linear activation function for the output neurons. Both types of functions complied with the differentiability conditions imposed by the training algorithm.

3.2. ANN training and prediction quality

One of the most relevant aspects of a neural network is its ability to generalize, that is, to predict cases that are not

Table 4: Optimum number of neurons for the ANN of each output.

Outputs	Units	No. of hidden layer	No. of neurons
Total friction loss	Watt	2 rpm	5
Friction loss due to damping effect	Watt	2 Pa s	8
Minimum oil film thickness (lower shell)	µm	2 N	9
Total oil consumption during one cycle	Liter/min	1 µm	10
Maximum eccentricity (lower shell)	–	2 mm	9
Oil temperature rise	°C	2	8
Maximum value of shell pressure	MPa	1	5

included in the training set. One of the problems that occur during neural network training is called overfitting. The error on the training set is driven to a very small value, but when new data is presented to the network, the error is large. The network has memorized the training examples, but it has not learned to generalize to new situations. One method for improving network generalization is to use a network that is just large enough to provide an adequate fit. The larger network you use, the more complex functions the network can create. There are two other methods for improving generalization that are implemented in MATLAB Neural Network Toolbox software: regularization and early stopping. More details about the generalization and regularization can be found in [29].

The typical performance function used for training feed forward neural networks is the mean sum of squares of the network errors.

$$mse = \frac{1}{N}\sum_{i=1}^{N}(e_i)^2 = \frac{1}{N}\sum_{i=1}^{N}\left(X_{\text{real}}(i) - X_{\text{predicted}}(i)\right)^2 .$$

It is possible to improve generalization, if you modify the performance function by adding a term that consists of the mean of the sum of squares of the network weights and biases.

$$msereg = \lambda mse + (1-\lambda) msw,$$

where λ is the performance ratio, and:

$$msw = \frac{1}{N}\sum_{j=1}^{N} w_j^2 .$$

Using this performance function causes the network to have smaller weights and biases, and this force the network response to be smoother and less likely to overfit.

Once the different stages of the training process and the ANN structure had been determined, and before the optimization procedure was developed, it was important to estimate the

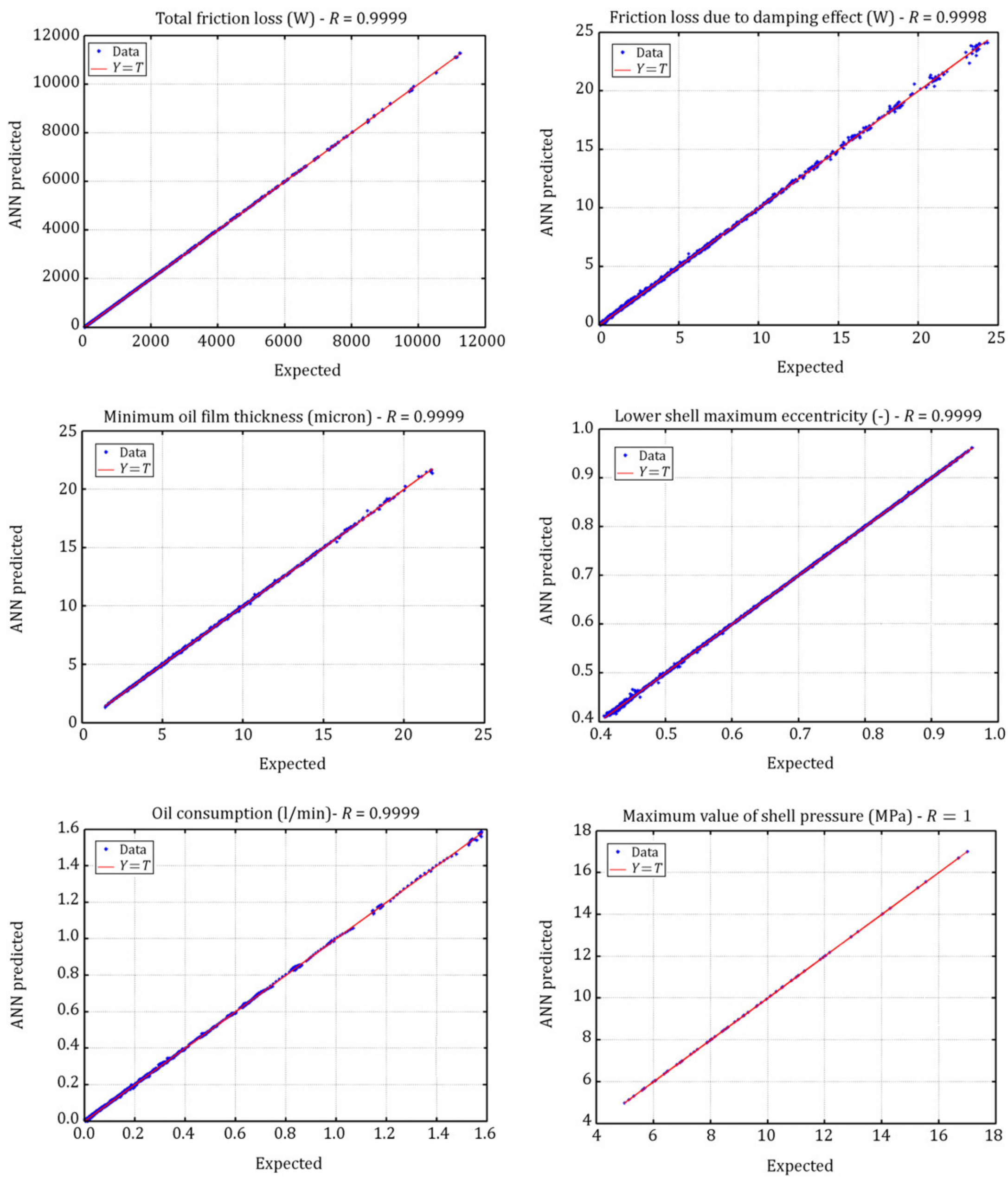

Figure 3: Prediction for each output.

ANN prediction qualities. Figure 3 shows some predicted output parameters plotted against the expected values for main bearing No. 1; an ideal 1:1 correlation falls on the solid line. The excellent agreement is evident in the figures. This close agreement shows that the ANN can be used in the data analysis of theoretical work to generate missing data in the theoretical program. The results of the model ANN are compared with the hydrodynamic simulation data. Figure 4 illustrate a comparison between the ANN results and the hydrodynamic simulation data of Minimum Oil Film Thickness (MOFT) for main bearing No. 1 in case of 5000 rpm, $D = 44$ mm, $L = 17.6$ mm, $F = 9.3$ kN and different oil viscosity. As can be seen, there is a good agreement between hydrodynamic simulation and predicted data.

Figure 5 illustrate a comparison between the ANN results and the hydrodynamic simulation data of total friction loss for main bearing No. 1 in case of 5000 rpm, $D = 44$ mm, $L = 17.6$ mm, $F = 9.3$ kN and different oil viscosity; they are in excellent agreement.

Figure 6 illustrate a comparison between the ANN results and the hydrodynamic simulation data of oil consumption during one cycle for main bearing No. 1 in case of 5000 rpm, $D = 44$ mm, $L = 17.6$ mm, $F = 9.3$ kN and different oil viscosity; they are in excellent agreement.

4. Optimization methodologies

GAs has traditionally been employed for optimization problems with objective functions that do not present continuity or differentiability properties [30]. It can be categorized into Single Objective Genetic Algorithm (SOGA) and Multi-Objective Genetic Algorithm (MOGA).

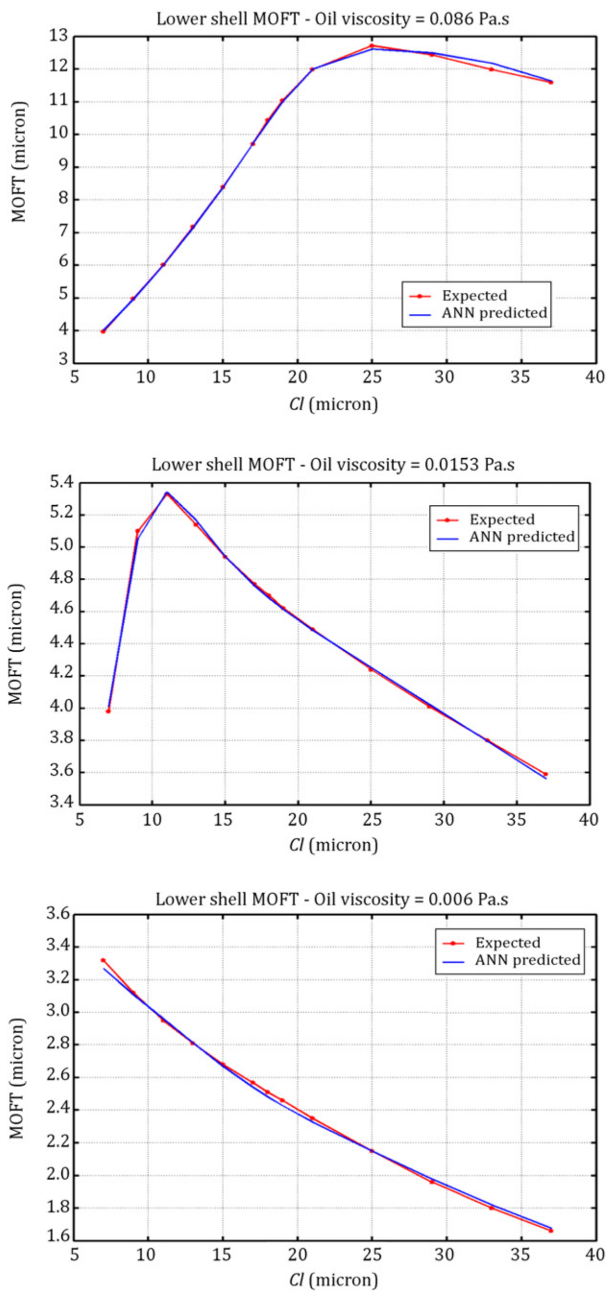

Figure 4: Comparison between the ANN results and the hydrodynamic simulation data of Minimum Oil Film Thickness (MOFT) for main bearing No. 1 in case of 5000 rpm, $D = 44$ mm, $L = 17.6$ mm, $F = 9.3$ kN and different oil viscosity.

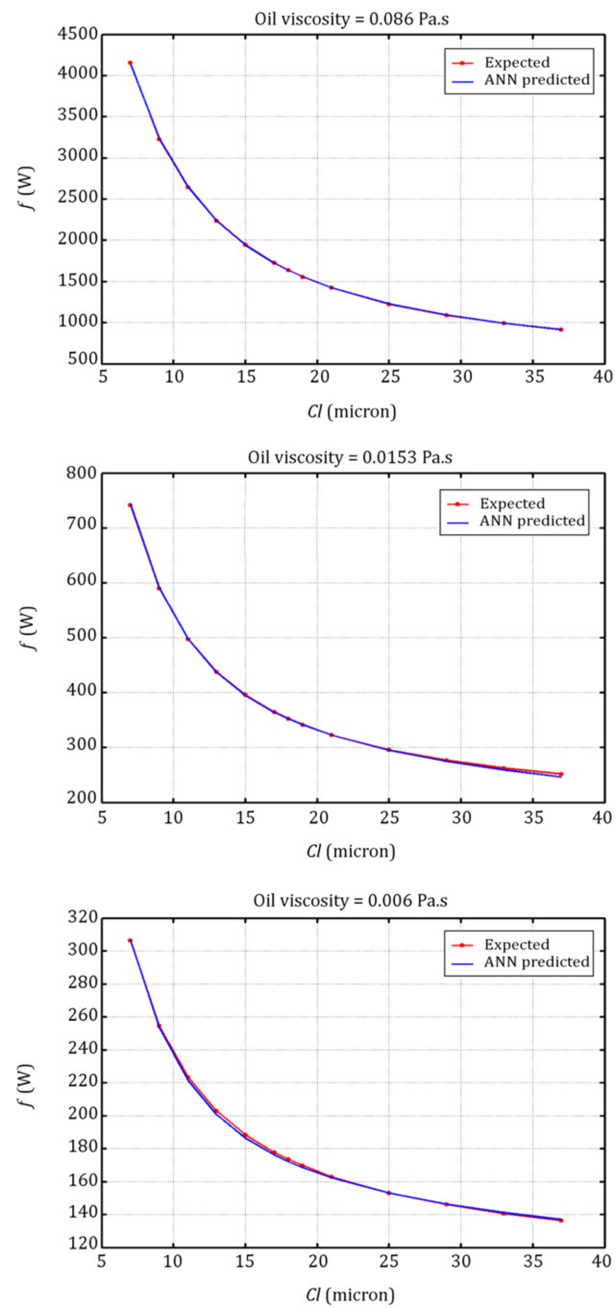

Figure 5: Comparison between the ANN results and the hydrodynamic simulation data of total friction loss for main bearing No. 1 in case of 5000 rpm, $D = 44$ mm, $L = 17.6$ mm, $F = 9310$ N and different oil viscosity.

According to the introduction, bearing optimization is naturally a multi-objective problem. Nevertheless, SOGA can still be employed for engine optimization by introducing a merit function of all the objectives [31,32]. However, these previous studies also showed that the results of SOGA depend on the definition of merit function, which is at times unclear prior to the optimization process. Therefore, MOGA is gaining popularity in engine optimization.

Instead of optimizing the merit function, as with SOGA, MOGA defines a so-called Pareto front, which consists of Pareto designs. A Pareto design is one that no other design has all objectives superior to it. For all designs $\vec{x}$ and corresponding N objectives, $f_k(\vec{x})$, $k = 1, 2, \ldots, N$, the Pareto design $\vec{x}^*$ is defined as follows: for an arbitrary design j, there exists at least one objective, k, that $f_k(\vec{x}) \geq f_k(\vec{x}^*)$ [33,34]. MOGA defines the Pareto front while maintaining diversity in the results. In the present work, a Non-dominated Sorting Genetic Algorithm II (NSGA-II) was employed [35]. According to the objectives, elitism is assigned to the designs. The designs with higher elitism have the priority to be selected for reproduction. If two designs have the same elitism, the one with higher crowding distance is assigned higher priority.

It should be noted that the optimization of the whole range of bearing operating conditions was not feasible due to the large number of parameters involved. Instead, this process was simplified by optimizing only a small number

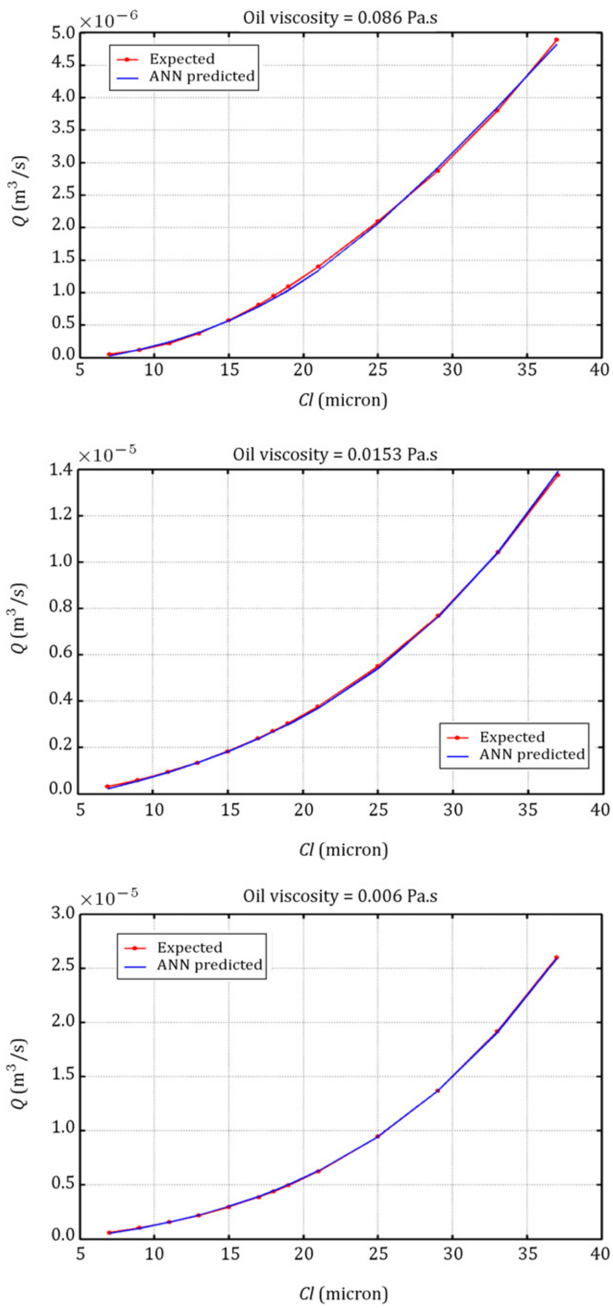

Figure 6: Comparison between the ANN results and the hydrodynamic simulation data of oil consumption during one cycle for main bearing No. 1 in case of 5000 rpm, $D = 44$ mm, $L = 17.6$ mm, $F = 9310$ N and different oil viscosity.

of particular bearing conditions (defined by engine speed, oil viscosity, maximum force applied on bearings, bearing radial clearance, bearing diameter and slenderness ratio). Hirani [19] in his paper dealt with multi-objective optimization (minimization of temperature rise, minimization of oil feed flow and minimization of power loss) and discrete design variables (lubricant viscosity, radial clearance and slenderness ratio) related to the design of a journal bearing. The results of his work led to the recommendation of using simultaneous minimization of oil flow and power loss and he indicated that the oil viscosity is of the highest importance of design variables.

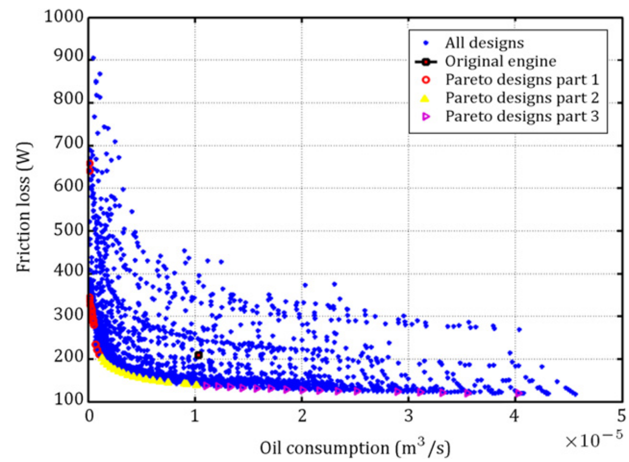

Figure 7: All and Pareto designs at $N = 5000$ rpm, $F = 9.3$ kN and $\mu = 0.006$ Pa s after 200 generation.

Hirani and Sue [20] selected five design variables (the radial clearance, slenderness ratio, oil viscosity, groove location and supply pressure) to control the bearing performance. They followed the previous work which had been done by Hirani [19]. Hirani and Sue chose the same objective function (oil flow and power loss) and used Axiomatic design to understand the bearing optimization problem in depth. They diagnosed redundancy (redundancy is reduced by using sensitivity analysis) and coupling in journal bearing design and observed negligible effect of supply pressure and groove, located in divergent region. Further, monotonic behavior of medium length of bearing was demonstrated.

4.1. Genetic algorithm

This section describes the details of the GA, fitted to solving bearing optimization problem. Three design variables, the radial clearance (Cl), bearing diameter (D) and slenderness ratio (L/D), are selected to control the bearing performance. The range of each variable is demonstrated in Table 3. We fixed the viscosity value; there are two reasons for that: first, for specified oil in IC engine, the oil temperature at actual operation condition is free running; second, we fix the oil viscosity at critical temperature (about 140 degree of centigrade) of lubrication system and the variation of viscosity value around this point is really small. According to Hirani and Sue's work [20], there is a negligible effect of supply pressure and groove, located in divergent region on bearing performance. Therefore, we omitted supply pressure, groove and viscosity from design variables.

Binary coding NSGA-II with five digits for each variable is chosen. Total population of 100 members, with crossover probability of 0.9 and mutation probability of 0.02 are considered. Constraint on minimum film thickness (to assure full hydrodynamic regime, MOFT ≥ 0.5 µm), and on maximum temperature rise (to limit the thermal thinning of lubricant, $\Delta T \leq 10$ °C) are imposed.

Figure 7 illustrates the results obtained for main bearing No. 1 at 5000 (rpm), Maximum force exerted on bearing equal to 9.3 kN and oil viscosity equal to 0.006 Pa s. Results of power loss and flow rate for Pareto design variables, along with minimum film thickness and temperature rise, are listed in Table 5.

Results of Table 5 are interesting to study. Understanding the effect of individual design variables (Cl, D and L/D ratio) on

Table 5: Pareto designs after 200 generations; $N = 5000$ rpm and $F = 9.3$ kN.

Parameters	f	Q	Cl	D	L/D	MOFT	DT
Original engine	210	1.03E–05	25	50	0.36	3	10.1
First part: Optimized engine has a friction loss value greater than real engine, but its oil consumption is lesser than real engine	659	1.39E–07	7.0	52	0.46	4.0	9.6
	641	1.49E–07	7.0	52	0.45	4.1	8.8
	345	1.49E–07	7.0	44	0.46	3.8	4.3
	337	1.51E–07	7.0	44	0.45	3.7	4.3
	328	1.92E–07	7.0	44	0.43	3.6	4.2
	320	2.73E–07	7.0	44	0.42	3.5	4.3
	316	3.17E–07	7.8	44	0.46	3.9	3.4
	309	3.20E–07	7.8	44	0.45	3.8	3.4
	301	3.62E–07	7.8	44	0.43	3.6	3.4
	294	4.43E–07	7.8	44	0.42	3.5	3.4
	292	4.97E–07	8.5	44	0.46	3.9	2.8
	286	5.01E–07	8.5	44	0.45	3.8	2.8
	280	5.44E–07	8.5	44	0.43	3.6	2.9
	234	6.79E–07	7.0	44	0.25	1.5	3.8
	222	8.50E–07	7.8	44	0.25	1.5	3.0
	211	1.05E–06	8.5	44	0.25	1.4	2.4
Second part: Both friction loss and oil consumption in optimized engine is lesser than real engine	202	1.27E–06	9.3	44	0.25	1.4	1.9
	194	1.52E–06	10.1	44	0.25	1.4	1.6
	187	1.80E–06	10.8	44	0.25	1.3	1.4
	181	2.12E–06	11.6	44	0.25	1.3	1.1
	176	2.46E–06	12.4	44	0.25	1.3	1.0
	171	2.85E–06	13.2	44	0.25	1.2	0.8
	167	3.27E–06	13.9	44	0.25	1.2	0.7
	163	3.73E–06	14.7	44	0.25	1.2	0.6
	159	4.24E–06	15.5	44	0.25	1.2	0.5
	156	4.79E–06	16.2	44	0.25	1.1	0.5
	153	5.39E–06	17.0	44	0.25	1.1	0.4
	150	6.04E–06	17.8	44	0.25	1.1	0.4
	148	6.74E–06	18.5	44	0.25	1.1	0.3
	145	7.49E–06	19.3	44	0.25	1.1	0.3
	143	8.99E–06	20.8	44	0.26	1.2	0.2
	141	9.18E–06	20.8	44	0.25	1.0	0.2
	139	1.01E–05	21.6	44	0.25	1.0	0.2
Third part: Optimized engine has a oil consumption value greater than real engine, but its friction loss is lesser than real engine	138	1.11E–05	22.4	44	0.25	1.0	0.2
	136	1.22E–05	23.2	44	0.25	1.0	0.2
	135	1.33E–05	23.9	44	0.25	1.0	0.1
	133	1.45E–05	24.7	44	0.25	0.9	0.1
	132	1.58E–05	25.5	44	0.25	0.9	0.1
	131	1.71E–05	26.2	44	0.25	0.9	0.1
	129	1.86E–05	27.0	44	0.25	0.9	0.1
	128	2.01E–05	27.8	44	0.25	0.9	0.1
	127	2.17E–05	28.5	44	0.25	0.9	0.1
	126	2.34E–05	29.3	44	0.25	0.8	0.1
	125	2.52E–05	30.1	44	0.25	0.8	0.1
	124	2.90E–05	31.6	44	0.25	0.8	0.1
	123	3.11E–05	32.4	44	0.25	0.8	0.1
	122	3.32E–05	33.2	44	0.25	0.8	0.1
	121	3.55E–05	33.9	44	0.25	0.8	0.1
	120	4.03E–05	35.5	44	0.25	0.7	0.1

power loss and oil flow is really essential and useful. Increase in bearing diameter and length increases friction loss, but increase in bearing radial clearance reduces friction loss. Similarly, increasing the bearing radial clearance and length increases the oil flow drastically. Thus, the optimization algorithm tries to find the smallest value of bearing diameter and length and largest value of bearing clearance to minimize the friction loss. On the other hand, minimizing the oil consumption forces the optimization algorithm to find out smallest value of bearing radial clearance and length. The data in Table 5 are divided into three parts, comparing the value of two objectives of optimized engine with original engine. First, friction loss of optimized engine is greater than same value in original engine, but oil consumption not. Second, both objectives in optimized engine are smaller than original engine. Third, oil consumption of optimized engine is greater than same value in original engine, but friction loss not.

As mentioned in previous paragraph, in the first part, optimized radialclearance falls in the range of 7–8.5 μm, even though selected design range was 7–37 μm and recommends L/D ratio of 0.42–0.46. In the second part, optimized radial clearance falls in the range of 9–22 μm and recommends L/D ratio of approximately 0.25. Similarly, in the third part, Table 5 recommends L/D ratio of approximately 0.25 and clearance falls in the range of 22–36 μm.

This design reduces the friction force to 28% in the third part of Table 5, and oil flow by 98% in the first part of Table 5. Ideally, a final decision for Cl, L/D and D needs to be taken depending on the importance of power loss and/or oil flow.

One can find results illustrated in Figure 7 and Table 5. Lower limit of bearing diameter equals 44 is selected for all designs except for two first designs. Furthermore, lower limit of L/D ratio equals 0.25 is selected in most designs especially for the second and third parts of Table 5. However, results of Table 5

Table 6: Pareto designs after 200 generations; $N = 6000$ rpm and $F = 8.2$ kN.

Parameters	f	Q	Cl	D	L/D	MOFT	DT
Original engine	307	1.07E−05	25	50	0.36	3.4	14.4
	284	1.59E−06	10	44	0.25	1.3	2.4
	274	1.87E−06	11	44	0.25	1.2	2.0
	266	2.18E−06	12	44	0.25	1.2	1.7
	252	2.91E−06	13	44	0.25	1.2	1.2
	247	3.33E−06	14	44	0.25	1.1	1.1
	242	3.79E−06	15	44	0.25	1.1	0.9
Optimized engine	233	4.84E−06	16	44	0.25	1.1	0.7
	229	5.43E−06	17	44	0.25	1.0	0.6
	225	6.07E−06	18	44	0.25	1.0	0.5
	222	6.75E−06	19	44	0.25	1.0	0.5
	218	8.23E−06	20	44	0.26	1.1	0.4
	215	9.03E−06	21	44	0.26	1.1	0.4
	213	9.89E−06	22	44	0.26	1.0	0.3

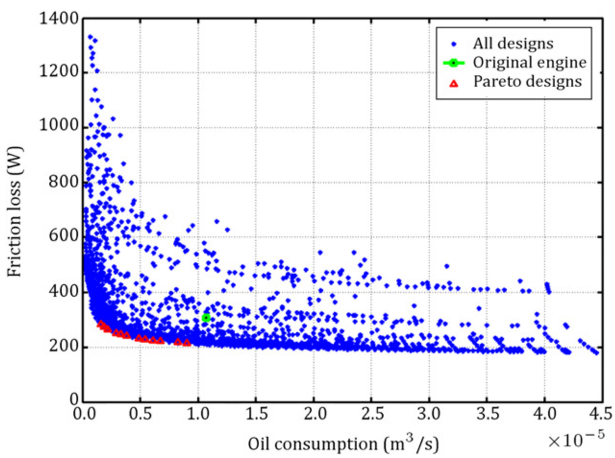

Figure 8: All and Pareto designs at $N = 6000$ rpm, $F = 8.2$ kN and $\mu = 0.006$ Pa s after 200 generation.

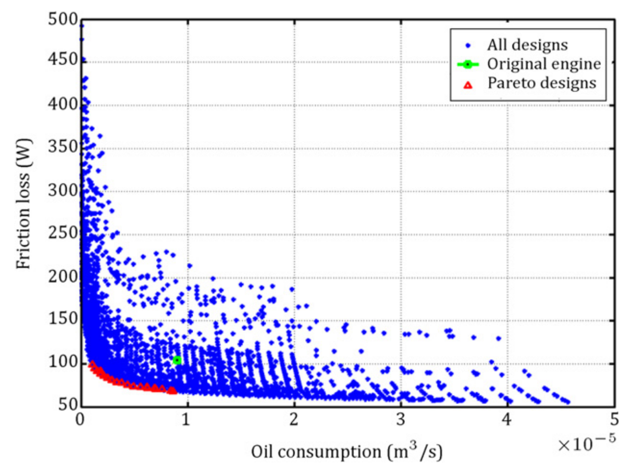

Figure 9: All and Pareto designs at $N = 3500$ rpm, $F = 13.2$ kN and $\mu = 0.006$ Pa s after 200 generation.

are optimized solutions, but they are not the best. To resolve this coupling, one needs to have a thorough understanding of some critical points in internal combustion engine design:

- Design variable L is determined based on the length of IC engine and the distance between cylinders. In order to compare the optimized results of journal bearing optimization to real data of original engine, the range of L should be limited. It can be done by exerting a constraint on lower limit of L.
- The lower limit of variable D is found out according to strength of materials analysis of crankshaft.
- The essential constraint which is missed here is load capacity. Finding this constraint needs to have a range of load capacity in IC engine bearings. Once the load capacity is determined in accordance with materials used in IC engine bearings, we can define the mentioned constraint in the terms of maximum force exerted on bearing per multiple of D and $L(F/(D.L))$. Hence, the optimized results will be more accurate.

The following illustrates bearing optimization methodology by two case studies: rated power and rated torque. According to the discussion in previous paragraph, the optimized results, in which both objective function values are smaller than the same value in original engine, are demonstrated.

4.2. Case study 1: rated power condition

For bearing engine speed = 6000 rpm, maximum force exerted on bearing = 8.2 kN and oil viscosity = 0.006 Pa s, the optimized results are listed in Table 6 and illustrated in Figure 8. These results are compared with simulation results of mentioned engine where clearance, bearing diameter and length were specified at Table 1. Observation of Table 6 and Figure 8 recommends clearance ranging from 10 to 22 μm and a slenderness ratio of approximately 0.25. This provides less oil leakage, reduced friction loss, insignificant temperature rise and tolerable minimum film thickness. This design reduces the friction force by 7%–44% and oil flow by 8%–85%.

4.3. Case study 2: rated torque condition

For bearing engine speed = 3500 rpm, maximum force exerted on bearing = 13.2 kN and oil viscosity = 0.006 Pa s, the optimized results are listed in Table 7 and illustrated in Figure 9. These results are compared with simulation results of mentioned engine where clearance, bearing diameter and length were specified at Table 1. Observation of Table 7 and Figure 9 recommends clearance ranging from 9 to 19 μm and a slenderness ratio of approximately 0.25. This design reduces the friction force to 32% and oil flow by 88%.

Table 7: Pareto designs after 200 generations; $N = 3500$ rpm and $F = 13.2$ kN.

Parameters	f	Q	Cl	D	L/D	MOFT	DT
Original engine	104	9.01E–06	25	50	0.36	3.3	5.7
Optimized engine	99	1.03E–06	9.3	44	0.25	1.5	1.2
	95	1.25E–06	10.1	44	0.25	1.5	1.0
	92	1.50E–06	10.8	44	0.25	1.4	0.8
	92	1.78E–06	11.6	44.5	0.25	1.5	0.7
	89	1.79E–06	11.6	44	0.25	1.4	0.7
	86	2.11E–06	12.4	44	0.25	1.4	0.6
	84	2.47E–06	13.2	44	0.25	1.4	0.5
	81	2.86E–06	13.9	44	0.25	1.4	0.4
	79	3.31E–06	14.7	44	0.25	1.4	0.4
	78	3.79E–06	15.5	44	0.25	1.3	0.3
	76	4.32E–06	16.2	44	0.25	1.3	0.3
	74	4.90E–06	17.0	44	0.25	1.3	0.2
	73	5.54E–06	17.8	44	0.25	1.3	0.2
	73	6.17E–06	18.5	44	0.26	1.4	0.2
	72	6.22E–06	18.5	44	0.25	1.3	0.2
	72	6.86E–06	19.3	44	0.26	1.4	0.2
	71	6.96E–06	19.3	44	0.25	1.3	0.1
	71	7.60E–06	20.1	44	0.26	1.4	0.1
	69	8.40E–06	20.8	44	0.26	1.4	0.1
	68	8.62E–06	20.8	44	0.25	1.2	0.1

5. Conclusion

The overall objective raised in this study integrates a problem of complex hydrodynamic modeling of journal bearings in internal combustion engines, together with an optimization process characterized by a high number of variables to be simultaneously modified and a high number of constraints to be satisfied. The scope of this paper is to evaluate the suitability of combining both ANN and NSGA-II techniques in this difficult and important task. The close agreement between expected and predicted data shows that the ANN can be used in the data analysis of theoretical work, to generate missing data in the theoretical program.

NSGA-II is used to optimize two objective functions under two constraints (temperature rise and minimum film thickness). The objectives, power loss and flow rate are functions of three variables: radial clearance, bearing diameter and slenderness ratio. Further, Pareto-optimal concepts are utilized to help the best situation between power loss and oil flow. These results are very encouraging and give a motivation for the use of the proposed optimization methodology, together with load capacity constraint in IC engine journal bearings. However, this requires a look up table of bearing materials and their load capacity.

Acknowledgment

The authors would like to thank Mr. Hossein Hashemi for his invaluable guidance.

References

[1] Ocvirk, F.W. "Short bearing solution approximation for full journal bearings", NACA. TN., 2808 (1952).
[2] Dubois, G.B., Ocvirk, F.W. and Wehe, R.L. "Experimental investigation of eccentricity ratio, friction, and oil flow of long and short journal bearings with load-number charts", NACA. TN., 3491 (1955).
[3] Campbell, J., Love, P.P., Martin, F.A. and Rafique, S.O. "Bearings for reciprocating machinery: a review of the present state of theoretical, experimental and service knowledge", *Proceedings of the Institution of Mechanical Engineers*, 182(3A), pp. 37–51 (1968).
[4] Martin, F.A. "Development in engine bearing design", *Int. J. of Tribology*, 16, pp. 147–164 (1983).
[5] Majumdar, B.C., *Dynamically Loaded Hydrodynamic Fluid Film Bearings; Status Report on Some Selected Topics in Theoretical and Applied Mechanics*, Indian National Science Academy pp. 57–64 (1994).
[6] Roshan, P., Singhasan, R. and Singh, D.V. "Analysis of a big end bearing — a finite element approach", *Wear*, 114, pp. 275–293 (1987).
[7] Booker, J.F. "Dynamically loaded journal bearings-mobility method of solution", *Transactions of the ASME, Journal of Basic Engineering, Series D*, 187, pp. 537–546 (1965).
[8] Paranjpe, R.S. and Goenka, P.K. "Analysis of crankshaft bearings using a mass conserving algorithm", *STLE Tribology Transactions*, 33, pp. 333–344 (1990).
[9] Goenka, P.K. "Analytical curve fits for solution parameters of dynamically loaded journal bearings", *ASME Journal of Tribology*, 106, pp. 421–428 (1984).
[10] Booker, J.F. "Dynamically loaded journal bearings: numerical application of mobility method", *ASME Journal of Lubrication Technology*, 93(1), pp. 168–176 (1971).
[11] Sanjay, D., Shrimpling, S. and Shrimpling, G. "Journal bearing analysis in engines using simulation techniques", SAE, 2003-01-0245, 2003.
[12] Reason, B.R. and Narang, I.P. "Rapid design and performance evaluation of steady state journal bearings — a technique amenable to programmable hand calculators", *ASLE Transactions*, 25, pp. 429–444 (1982).
[13] Hirani, H., Athre, K. and Biswas, S. "Rapid and globally convergent method for dynamically loaded journal bearing design", *Proceedings of the Institution of Mechanical Engineers, Part J*, 212, pp. 207–214 (1998).
[14] Stahl, J. and Jacobson, B.O. "Design functions for hydrodynamic bearings", *Proceedings of the Institution of Mechanical Engineers, Part J*, 215, pp. 405–416 (2001).
[15] Howlett, R.J., Zoysa, M.M., Walters, S.D. and Howson, P.A. "Neural network techniques for monitoring and control of internal combustion engines", in: *Proc. Int. Symp. Intell. Ind. Autom.* (1999).
[16] Hashimoto, H. "Optimum design of high-speed, short journal bearings by mathematical programming", *Tribology Transactions*, 40, pp. 283–293 (1997).
[17] Hashimoto, H. and Matsumoto, K. "Improvement of operating characteristics of high-speed hydrodynamic journal bearing by optimum design: Part I—formulation of methodology and its application to elliptical bearing design", *Transactions of the ASME, Journal of Tribology*, 123(2), pp. 305–312 (2001).
[18] Wang, N., Ho, C.I. and Cha, K.C. "Engineering optimum design of fluid film lubricated bearings", *STLE Tribology Transactions*, 43(3), pp. 377–386 (2000).
[19] Hirani, H. "Multiobjective optimization of a journal bearing using the Pareto optimal concept", *Journal of Engineering Tribology, Proceedings of the Institution of Mechanical Engineers, Part J*, 218, pp. 323–336 (2004).
[20] Hirani, H. and Suh, N.P. "Journal bearing design using multiobjective genetic algorithm and axiomatic design approaches", *Int. J. of Tribology*, 38, pp. 481–491 (2005).
[21] Zengeya, M. and Gadala, M. "Optimization of journal bearings using a hybrid scheme", *Int. J. of Tribology*, 221, pp. 591–607 (2007).
[22] Hamrock, B.J., *Fundamentals of Fluid Film Lubrication*, McGraw Hill, New York (1994).
[23] Lennox, B., Montague, G.A., Frith, A.M., Gent, C. and Bevan, V. "Industrial applications of neural networks: an investigation", *Journal of Process Control*, 11, pp. 497–507 (2001).

[24] Ozmutlu, H.C., Fatih, C. and Ozmutlu, S. "Cross-validation of neural network applications for automatic new topic identification", *Journal of the American Society for Information Science and Technology*, 59(3), pp. 339–362 (2008).
[25] Haykin, S., *Neural Networks*, Macmillan College Publishing, Englewood Cliffs, NJ (1994).
[26] Alonso, J.M., Fernando, A., Desantes, J.M., Hernández, L., Hernandez, V. and Molto, G. "Combining neural networks and genetic algorithms to predict and reduce diesel engine emissions", *IEEE Transaction on Evolutionary Computation*, 11(1), pp. 46–55 (2007).
[27] Zurada, J.M., *Introduction to Artificial Neural Systems*, PWS Publishing, Boston, MA (1992).
[28] Maren, A.J., Herston, C.T. and Pap, R.M., *Handbook of Neural Computing Applications*, Academic, Ed, New York (1990).
[29] The Math Works, Inc. "Neural network toolbox for use with MATLAB", User's Guide releases (2007).
[30] Davis, L., *The Handbook of Genetic Algorithms*, Van Nostrand Reingold, New York (1992).
[31] Kim, M., Liechty, M.P. and Reitz, R.D. "Application of micro-genetic algorithms for the optimization of injection strategies in a heavy-duty diesel engine", SAE, 2005-01-0219 (2005).
[32] Sun, Y. and Reitz, R.D. "Modeling diesel engine NO_x and soot reduction with optimized two-stage combustion", SAE, 2006-01-0027 (2006).
[33] De-Risi, A., Donateo, T. and Laforgia, D. "Optimize of the combustion chamber of direct injection diesel engines", SAE, 2003-01-1064 (2003).
[34] Hai-Wen, G., Shi, Y. and Reitz, D. "Heavy-duty diesel combustion optimization using multi-objective genetic algorithm and multi-dimensional modeling", SAE, 2009-01-0716 (2009).
[35] Deb, K., Pratap, A., Agarwal, S. and Meyarivan, T. "A fast elitist multi-objective genetic algorithm, NSGA-II", *IEEE Transactions, Evolutionary Computation*, 2, pp. 182–197 (2002).

Jafar Ghorbanian received his B.S. degree in fluid mechanics from Amirkabir University in 2004, Tehran, Iran and his M.S. degree in mechanical engineering from K.N. Toosi university of Technology, Tehran, Iran 2007. His research interests are thermo-fluids, heat transfer, IC engines, CFD and applied intelligence. He is now working at IPCO.

Mahdi Ahmadi received his B.S. degree in fluid mechanics from Amirkabir University in 2005, Tehran, Iran. He is now head of the department of CAE at IPCO.

Reza Soltani received his B.S. and M.S. degrees in mechanical engineering from K.N. Toosi University of Technology in 2000 and 2002, respectively. His major research interests lie in CFD and Tribology (Friction, Wear and Lubrication) in internal combustion engines. He is working at IPCO which is the number one in Middle-East automotive industry.